CO oxidation on a Au/TiO_2 nanoparticle catalyst via the Au-assisted Mars - van-Krevelen mechanism

Philomena Schlexer[a,#], Daniel Widmann[b], R. Jürgen Behm[b,*], Gianfranco Pacchioni[a]

[a] Dipartimento di Scienza dei Materiali, Universitá Milano-Bicocca, I-20125, Italy

[b] Institute of Surface Chemistry and Catalysis, Ulm University, D-89069 Ulm, Germany

Abstract

Recently, there has been increasing evidence that CO oxidation on TiO_2 supported Au catalysts proceeds via a Au-assisted Mars – van Krevelen mechanism for reaction temperatures above room temperature. We here present results of a combined experimental and theoretical study, aiming at the identification of activated steps in this reaction. O_2 multi-pulse experiments, performed in a temporal analysis of products (TAP) reactor at different temperatures between -80°C and 240°C, revealed that the replenishment of surface lattice oxygen vacancies at perimeter sites, at the perimeter of the interface between TiO_2 support and Au nanoparticles, proceeds with essentially constant efficiency, independent of the reaction temperature. Hence, this reaction step is barrier-free. Previous studies (*D. Widmann and R.J. Behm, Angew. Chem. Int Ed. 50 (2011) 10241*) had shown that the preceding step, the formation of a surface lattice oxygen vacancy at these sites, is activated, requiring temperatures above room temperature. Density functional theory based calculations, performed on a Au nano-rod supported on a TiO_2 anatase (101) substrate confirmed that the presence of the Au nano-rod leads to a significant reduction of the vacancy formation energy at these sites, resulting in a barrier of only ~0.9 eV for vacancy formation by reaction with adsorbed CO. The reverse process, replenishing the vacancies by reaction with O_2, was found to be activated in the case of individual vacancies, but essentially barrier-free for the case of pairs of neighbored vacancies. Consequences of these findings for the mechanism of the CO oxidation reaction on these catalysts, which can be considered as a model system for Au catalysts supported on reducible oxides, are discussed.

Submitted to ACS Catal.: 18.01.2018

* Author to whom correspondence should be addressed, email: juergen.behm@uni-ulm.de

Pres. Address: SUNCAT Center for Interface Science and Catalysis, Dept. of Chemical Engineering, Stanford University, Stanford, CA 94305, USA

1 Introduction

Au catalysts consisting of small Au nanoparticles supported on various metal oxides have attracted considerable attention in the past 30 years due to their high activity for catalyzing various oxidation and reduction reactions already at rather low temperatures. [1-4] Examples include, e.g., the CO oxidation,[5-9] the water-gas shift reaction,[10-15] the selective and total oxidation of hydrocarbons,[16-18] or hydrogenation reactions.[19-23] Among these, the oxidation of CO represents the by far most often investigated reaction, and often serves as a prototypical reaction for heterogeneously catalyzed reactions in general.[24] For the latter reaction, a number of experimental (for recent examples see, e.g., refs. [9;25-36]) and theoretical (for recent examples see, e.g., refs. [37-49]) studies could provide a rather detailed, but also contradictory picture of the surface processes contributing to the overall reaction, where the key factors are as follows: i) Under typical reaction conditions, at room temperature and above, CO is mainly adsorbed on the Au nanoparticles (NPs), while at lower temperatures it is also adsorbed on the oxide support. For reaction at very low temperatures <-130°C, the latter CO_{ad} species were shown to represent the reactive species because of the too low surface mobility of CO_{ad} on the Au nanoparticles ((NPs).[29] ii) For reaction at low temperatures, below room temperature, desorption of CO_2 product molecules becomes increasingly rate limiting, where the exact temperature depends on the respective oxide support.[50;51] iii) Most controversially discussed is the activation of molecular O_2. In most cases, the reaction was suggested to proceed via an adsorbed [O-O_{ad}···CO_{ad}] intermediate,[38] where different sites were proposed as active sites, either undercoordinated Au atoms of the Au cluster ('gold only pathway' [38]) or sites at the perimeter of the interface between support and Au NPs ('perimeter sites'), where $O_{2,ad}$ was stabilized by additional interaction with the oxide support ('interface pathway' [38]). In a combined experimental and theoretical study, Green et al. could provide compelling evidence that for reaction at low temperatures (<145 K) CO_{ad} pre-adsorbed on the TiO_2 support reacts with $O_{2,ad}$ species adsorbing from the gas phase at the perimeter sites.[29]. On the other hand, Widmann et al. provided equally convincing evidence in a series of quantitative temporal analysis of products (TAP) reactor studies [30;33;52;53] that surface lattice oxygen species located at the support perimeter sites directly participate in the reaction at temperature of about 80°C and above, and proposed this as the dominant reaction pathway for reaction under these conditions. In that picture, surface lattice oxygen close to the Au NPs represents the active oxygen species for CO oxidation (O_{act}), which reacts with CO adsorbed on the Au NPs. Accordingly, the reaction proceeds via the continuous formation and replenishment of surface oxygen vacancies by reaction of the catalyst with CO and O_2, which was termed as Au-assisted Mars - van Krevelen mechanism.[30;33] A reaction mechanism involving oxygen vacancy formation was concluded also by Maeda et al. based on electric conductivity measurements.[31]

In the meantime, this mechanistic proposal for the CO oxidation on Au/TiO_2 has been supported also by results of other experimental studies, applying different techniques such as electrical conductivity or electron paramagnetic resonance (EPR) measurements.[35;54] Further studies indicated that also other Au catalysts based on reducible supports (Au/CeO_2, Au/Fe_xO_y, Au/ZrO_2, and Au/ZnO) operate in the same way for reaction above room temperature.[53;55;56] The field has been recently reviewed.[57]

Moreover, there is also evidence from several theoretical studies that the CO oxidation at ambient temperature and pressure on Au catalysts based on reducible metal oxide supports proceeds predominantly via such a redox mechanism, which includes the continuous and, on a molecular scale, alternating reduction and re-oxidation of the metal oxide support at the perimeter of the interface between the metal oxide and the Au NPs.[40;43;45;48] Using a Au_{10} cluster on a TiO_2 anatase (001) support, Saqlain et al calculated activation energies of 1.2 eV for reaction of CO_{ad} with surface lattice oxygen and of 0.35 eV for replenishment of the resulting vacancy by reaction with O_2.[48]

A third alternative was proposed by Vilhelmsen and Hammer.[41;44] Based on very detailed DFT calculations they proposed that the interface between Au nanoparticle and TiO_2 substrate is largely oxidized, and that this enhances the activity for O_2 dissociation at the perimeter sites of the oxidized interface. This results in adsorbed atomic oxygen, which can then react with CO to form CO_2. Rather similar conclusions were arrived at by Duan and Henkelman for a model catalyst consisting of TiO_2 rutile (110) with a Au nanorods deposited thereon.[47] They found that a specific site at the interface, the Au-Ti_{5c} site, allows facile dissociation of molecular O_2 with an activation barrier of 0.5 eV, and that the resulting atomic oxygen species can react with CO with a barrier of 0.25 eV, representing a Langmuir-Hinshelwood mechanism. Alternatively, CO_{ad} could react with surface lattice oxygen with a barrier of about 0.55 eV, which would be part of a Au-assisted Mars – Krevelen mechanism.

Further mechanistic information was derived from a combined TAP reactor and EPR study on the reactive removal of TiO_2 surface lattice oxygen (from Au/TiO_2) by CO.[35] Measurements performed at various temperatures between -90 °C and +120 °C clearly demonstrated that the removal of O_{act} is increasingly inhibited with decreasing reaction temperature, very low at -20°C and not at all possible any more at temperatures of -90°C. Hence, TiO_2 surface lattice oxygen cannot represent any more the active oxygen species at these low temperatures, and there has to be a change in the dominant reaction pathway with decreasing reaction temperature.[35] This also fits to previous findings on the dominant reaction pathway for the CO oxidation on Au/TiO_2 at much lower temperatures (down to -150 °C) by Green et al., who showed that under these conditions molecularly adsorbed oxygen represents the active oxygen species, forming a $[CO{\cdot}O_2]$ co-adsorption complex.[34] Although it is evident from these findings that the removal of TiO_2 surface lattice oxygen is an activated process, there is still no experimental proof that this indeed represents the rate determining step in the CO oxidation reaction for room temperature and higher, as it was proposed previously.[33] So far the activation barriers for the individual reaction steps are still unknown and it is not yet clear, whether the removal of active oxygen by CO or its formation, via the replenishment of surface oxygen vacancies by O_2 from the gas phase, is rate determining. Comparing with previous theoretical studies it is in particular unclear whether the preference for a Au-assisted Mars –van Krevelen mechanism is an artifact caused by the use of small Au clusters, or whether a such mechanism would also work for a more realistic Au/TiO_2 model system, and with activation barriers compatible with experimental data. Furthermore, it is particularly important to consider the full catalytic cycle, rather than focusing on specific reaction steps.[40;43;45]

These questions about the activated steps in the reaction are addressed in the present

combined experimental and theoretical study, employing TAP reactor measurements and density functional theory (DFT) based computations. TAP reactor measurements are particularly suited for such kind of studies since they allow to separate catalyst reduction and oxidation steps. After a brief description of the experimental procedures and theoretical methods (section 2), we first focus on the formation of surface lattice oxygen vacancies at the perimeter sites (section 3.1). This includes multi-pulse experiments in the TAP reactor, exposing the Au/TiO_2 catalyst alternately to sequences of multiple CO/Ar or O_2/Ar pulses in order to reactively remove and replenish the O_{act} species, respectively, at 240°C. Furthermore, it is important to note that all experiments were performed under completely dry conditions, to exclude any effects that could result from trace impurities of water.[32;58] On the theoretical side, we calculated the oxygen vacancy formation energy, both in the absence and presence of Au nanoparticles, and the pathway for lattice surface oxygen abstraction, including also the kinetic barriers in the individual steps. In the next section (section 3.2), we deal with the re-oxidation of the oxygen surface vacancies by reaction with adsorbed O_2. Experimentally, this was explored by exposing the pre-reduced catalyst (see above) to O_2 pulse sequences at different temperatures. The temperature dependence of the re-oxidation kinetics provides information on a possible activation energy in this reaction step, revealing whether (and to which extent) also the re-oxidation is an activated process. This is followed by calculations of the re-oxidation pathway, similar to those described above for O vacancy generation. The results are summarized in full catalytic cycles. Consequences of these findings for our understanding of the dominant reaction pathway on Au/TiO_2 at room temperature and above, and in particular whether the removal of TiO_2 surface lattice oxygen by CO is the rate determining step rather than re-oxidation by O_2 or CO_2 desorption, will be discussed.

2 Methodology

2.1 Experimental details

Temporal analysis of products (TAP) measurements were performed using a micro-reactor containing a commercial Au/TiO_2 catalyst from STREM Chemicals. The catalyst consists of Au nanoparticles with 1.0 % wt. Au loading, supported on non-porous TiO_2 from Degussa (P25, ca. 50 $m^2\ g_{cat}^{-1}$). The TiO_2 from Degussa contains around 80-90% anatase, and the rest is rutile.[59] The catalyst was pre-treated in a 20 Nml min^{-1} Ar gas flow at 100°C for 15 h, passing a moisture filter to ensure dry conditions. This sample was then calcined in 10% O_2/N_2 at 400°C for 30 min. A mean Au particle diameter of 2.9 ± 0.7 nm was determined by transmission electron microscopy (TEM) measurements after calcination. After cooling the catalyst to 120°C in a flow of Ar, the micro-reactor was evacuated at 120°C. Subsequently, the TAP measurements were conducted by exposing the calcined catalyst alternatingly to sequences of multiple CO/Ar and O_2/Ar pulses (CO/Ar = O_2/Ar = 1/1). One pulse typically contains between $2 \cdot 10^{15}$ and $8 \cdot 10^{15}$ molecules. Reduction of a fully oxidized Au/TiO_2 catalyst by CO/Ar pulses was always realized at 240°C, the highest temperature used for pulse experiments in this study. After removal of all available active oxygen species (O_{act}) by CO at 240°C, the sample was then rapidly cooled to the desired temperature for re-oxidation (between -80°C and 240°C) in vacuum, and exposed to O_2/Ar pulses. A detailed description of the TAP reactor can be found in ref. [60].

2.2 Computational details

Periodic, spin polarized density functional theory (DFT) calculations were performed using the Vienna Ab Initio Simulation Package (VASP 5.2).[61-64] Generalized gradient approximations (GGA) for the exchange-correlation functional were applied within the Perdew, Burke and Ernzerhof (PBE) formulation.[65;66] To circumvent the self-interaction error of the GGA functional, we used the GGA+U approach developed by Dudarev et al.[67] With this approach, the multiple occupation of d orbitals is penalized, so that the underestimation of the band gap and electron delocalization is attenuated. In this work, we set the U-parameter to 3 eV for the 3d levels of Ti. A U value of 2-3 eV for the Ti 3d levels has been proposed by Hu et al. to calculate reaction energies on titania.[68] The parameter provides a good qualitative description of electronic and geometric structures.[69] To describe electron – ion interactions, the projector augmented wave (PAW) method was used.[70;71] C(2s, 2p), O(2s, 2p), Ti(3s, 4s, 3p, 3d), and Au(5d, 6s) states were treated explicitly. For electronic relaxations, we used the blocked Davidson iteration scheme.[72;73] During structure optimizations, all ions were allowed to relax until ionic forces were smaller than |0.01| eV $Å^{-1}$.

Calculations of the titania anatase bulk structure was done using a kinetic energy cut-off of 900 eV. A Γ-centered K-point grid in the Monkhorst–Pack scheme [74] was used, which was set to (8×8×4). With this computational setup we obtain lattice parameters of a_0 = 3.803 Å and c_0 = 9.717 Å, compared with the corresponding experimental values [75] a_0 = 3.796 Å and c_0 = 9.444 Å. The deviation of the unit cell volume is 3.27%.

To model the titania anatase (101) surface we used slabs with 5 layers of TiO_2. The slabs were separated by more than 12 Å of vacuum and all ions were allowed to relax during structure optimizations. Depending on the system, we used (2×1) or (2×2) surface super-cells. Γ-point calculations were performed for the structure optimization and wave functions were expanded in the plane wave basis up to a kinetic energy of 400 eV. Dispersion forces can be important for the description of the cluster-support interaction.[76;77] Therefore, we used the semi-empirical dispersion correction proposed by Grimme known as the DFT-D2 approach.[78] It is generally assumed that the DFT-D2 method produces an overestimate of the dispersion interactions. For this reason we changed the parameters C_6 and R_0 of the DFT-D2 approach, as suggested by Tosoni and Sauer.[79] We denote this method as DFT-D2'. To construct the surface, we used the bulk lattice parameters obtained with DFT without vdW-correction, which is justified by the fact that the unit cell volumes of the bulk materials change by much less than 1%.

Au nanoparticles were modeled using Au nano-rods which are periodic in one direction of the titania surface unit cell. Here we considered two different Au nano-rod models: Au_{10}/TiO_2 and Au_{24}/TiO_2 (Table S1 and Fig. S1, Supporting Information). The Au_{10} rod was positioned onto the TiO_2(2×1) and the Au_{24} rod was positioned onto the TiO_2(2×2) unit cell. The rods and the unit cells of the rods were then optimized without the titania support, respectively. The resulting lattice parameters in the direction of the rods periodicity are shown in Table 1. The lattice mismatch between the nano-rod and the support results in a strain on the rod, because the lattice parameters of the support were kept fixed. The deviation of the lattice parameter of the free-standing rod from the TiO_2 lattice parameters is a measure for strain. This deviation is reported in Table 1. The strain is relatively small, about 1.2-1.3 %.

Table 1: Lattice parameters and strain of the nano-rods consisting of N Au atoms. $a_0(TiO_2)$ is the TiO_2 lattice parameter in the direction of the rod's periodicity. $a_0(Au_N, gas)$ is the optimized lattice parameter of the free-standing rod. N is the number of Au atoms.

	N	$a_0(TiO_2)$ [Å]	$a_0(Au_N, gas)$ [Å]	Deviation [%]
(2×1)	10	7.69	7.60	-1.2
(2×2)	24	7.69	7.79	+1.3

Adsorption energies were calculated as defined in eqn. (1), where N, the number of gold atoms in the supported nano-rods, is 10 or 24. E(X) denotes the total energy of the system X. All components refer to optimized systems. The vacancy formation energy is defined in eqn. (2). For the Au-free surface, we can formally set N = 0. For the oxidation of CO with oxygen from the TiO_2 lattice, the reaction energy can be calculated as shown in eqn. (3).

$$E_{ads}(Au_N/TiO_2) = E(Au_N/TiO_2) - E(Au_N) - E(TiO_2) \quad (1)$$

$$E_{Vo}(Au_N/TiO_2) = E(Au_N/TiO_{2-x}) + \frac{1}{2}E(O_2) - E(Au_N/TiO_2) \quad (2)$$

$$E_{REA} = E(CO_2) + E(Au_N/TiO_{2-x}) - E(CO) - E(Au_N/TiO_2) \quad (3)$$

Atomic charges q were estimated via the Bader decomposition scheme.[80;81] To determine CO stretching frequencies, harmonic force constants were calculated using the central finite difference method with 0.02 Å displacements in every Cartesian direction. The atoms of the CO molecule and the Au atom directly connected to CO were allowed to move. No imaginary frequencies were obtained. Scaled frequencies are defined in eqn. (4), where $\nu(CO_g)$ = 2126 cm^{-1} and $\nu^{exp}(CO_g)$ = 2143 cm^{-1}:

$$\nu^{SC} = \nu(CO)\nu^{exp}(CO_g)/\nu(CO_g) \quad (4)$$

To determine transition states we used the climbing-image nudged elastic band (CI-NEB) method.[82] In the CI-NEB calculations, images were optimized to obtain the minimum energy path until forces on ions were smaller than |0.05| eV/Å. We did not include zero-point energy corrections, because they are assumed to be negligible compared to other approximations inherent to the models used.

3 Results

3.1 CO oxidation with lattice oxygen from TiO_2

The oxidation of CO via the Au-assisted Mars-van Krevelen mechanism can be divided into two parts.[30;33] The first part is the reduction of the catalyst by surface lattice oxygen abstraction, due to reaction with CO, the second step is the re-oxidation of the catalyst by reaction of the vacancy with molecular oxygen. The catalyst is reduced by CO under formation of CO_2 according to reaction (5) and re-oxidized according to reaction (6).[35]

$$CO + Au/TiO_2 \rightarrow CO_2 + Au/TiO_{2-x} \quad (5)$$

$$O_2 + Au/TiO_{2-x} \rightarrow Au/TiO_2 + O_{ad} \quad (6)$$

In the second reaction, one oxygen atom of the adsorbed O_2 molecule remains on the surface and can subsequently either react with another vacancy or with a second CO molecule. Temporal analysis of products (TAP) measurements of the reduction and re-oxidation of the Au/TiO_2 catalyst were performed. As described in section 2, the catalyst was first exposed to CO/Ar pulses at 240°C (Fig. 1). In agreement with previous findings at T ≥ 80°C,[30] CO_2 is readily formed (note: the resulting CO_2 pulses are not shown). CO_2 formation was only observed during CO pulses, and the total amount of CO_2 formed equals the total amount of CO consumed during the whole sequence of CO/Ar pulses ($2.7 \cdot 10^{18}$ molecules g_{cat}^{-1}). In previous studies we have shown that the total amount of CO consumed / CO_2 formed decreased at lower temperatures and is finally inhibited at around -20°C and below, indicating that the removal of active oxygen from the catalyst surface (catalyst reduction) is an activated process.[30;35]

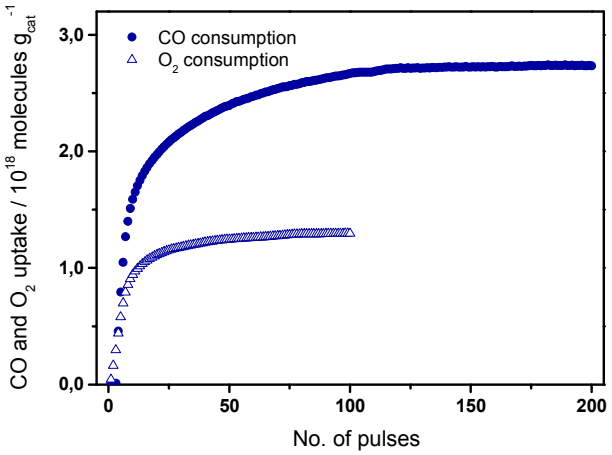

Fig. 1: Accumulated amounts of CO and O_2 consumption during reduction (CO/Ar pulses) and re-oxidation (O_2/Ar pulses) of Au/TiO_2 at 240°C.

Note that no CO_2 formation is observed upon exposure of the pristine titania surface to CO pulses, showing the important role of the Au nanoparticles for the catalyst reduction step.[30] This is in good agreement with results of our DFT calculations, which show that the oxidation of CO by reaction with the pristine TiO_2 anatase surface is endothermic by at least 1.3 eV (see below). Hence, the reaction barrier is likely to be even higher.

Assuming hemispherical Au particle shapes, and considering the Au loading and the Au particle size distribution, one can calculate that for a completely surface reduced Au/TiO_2 sample (all reactive surface lattice oxygen atoms are removed), after removal of $2.4 \cdot 10^{18}$ O atoms g_{cat}^{-1} by CO at 240°C (see above), the local vacancy coverage at the interface between Au and the TiO_2 support (relative to the total amount of O surface lattice atoms on perimeter sites) is about 135%. Hence, in accordance to previous results on a similar Au/TiO_2 catalyst, the local vacancy concentration at 240°C for a fully reduced catalyst sample is higher than 100%.[30] This clearly shows that in addition to all available active TiO_2 surface lattice oxygen

at the Au-TiO_2 perimeter sites, additionally also oxygen from neighboring sites was removed. In our previous studies we had assigned this to the mobility of TiO_2 surface lattice oxygen / surface oxygen vacancies at elevated temperatures (for $T \geq 160°C$).[33]

To determine the role of Au in the reduction of the titania substrate, we investigated the formation of oxygen vacancies in the vicinity of the Au nano-rod theoretically. First of all, these calculations reveal that the oxygen vacancy formation energy and hence also the CO oxidation energy is reduced by up to 2.2 eV when the O atom is removed in the vicinity of the Au rods (Table S1 and Fig. S1, Supporting Information). The reactive formation of the vacancy V_O 1–a under the bigger Au rod (Fig S1 (b), Supporting Information) is even exothermic, with a CO oxidation reaction energy of -0.44 eV. This vacancy is, however, located under the rod and is thus not easily accessible for abstraction by reaction with CO. The stabilization of the vacancies is related to a charge transfer from the vacancy to the Au rod, when the Au rod is close to or above the vacancy. The transferred electronic charge is mainly localized on the Au atom(s) close(r) to the vacancy. The ability of the Au rod to accept and stabilize excess electrons makes the Au/TiO_2 system more easily reducible than the Au-free TiO_2 substrate. Therefore, the stabilization of oxygen vacancies by the Au rods makes the CO oxidation step roughly thermo-neutral on A<u/TiO_2 anatase (101). With increasing vacancy concentration at the Au – TiO_2 interface perimeter, the Au particles should become more and more negatively charged at the perimeter. At high vacancy perimeter concentrations, the negative charge may become more delocalized in the Au particle due to the charge repulsion. In fact, we previously observed a red-shift of the CO stretching frequency by about 40 cm^{-1} after extensive reduction of the catalyst, indicating a negative charging of the Au particles. Similar observations were reported also for CO on small Au clusters, if these were deposited, e.g., on F-centers on MgO [83] or for small Au clusters on thin, metal supported MgO films.[84]

The above calculations clearly illustrate the effective enhancement of the catalyst reducibility by the presence of the Au particles. The ability of the Au particles to capture the excess electrons associated with the vacancies formed at the Au/TiO_2 perimeter leads to a stabilization of the vacancies. In the literature, also a different mechanism for the vacancy stabilization has been proposed, namely the oxidation of the Au/TiO_2 perimeter.[43;47;49] In that case, the Au/TiO_2 perimeter is highly oxidized, leading to only partly reduced oxygen adatoms with a net charge of less than -2 |e|. These oxygen atoms are able to capture excess electrons from the vacancies. The oxidation of the Au/TiO_2 rutile (110) interface was reported to be exothermic.[41;43;44;47;49] The thermodynamic stabilization of vacancies and simultaneously also the decrease of the kinetic barrier for oxygen abstraction at the Au/TiO_2 rutile (110) perimeter reported by Saqlain et al. [48] is most likely transferable to the TiO_2 anatase (101) surface. According to our computations, the adsorption of an oxygen adatom (O_{ad}) at the Au/TiO_2 anatase (101) perimeter is exothermic by around 1.8 eV with respect to ½ O_2. However, a substantial amount of interfacial adatoms (O_{ad}) (up to almost 1 ML with respect to the interfacial Au-Ti_{5c} sites) is needed to obtain a significant effect on the oxygen vacancy formation,[47] and during reaction the adatoms may be consumed by oxygen vacancies under reactive conditions. In the following we will therefore ignore the effect of interfacial oxygen adatoms on the vacancy formation.

To investigate the mechanism of the catalyst reduction, we first explored the adsorption of CO on the Au catalyst. We tested whether the presence of oxygen vacancies has an impact on the CO adsorption energy by considering stoichiometric and reduced titania supports. The reduced titania support contained a single surface oxygen vacancy per unit cell. This way we model a low to intermediate oxygen vacancy concentration at the Au perimeter (max. 25% of the O 2c perimeter sites). CO is preferably adsorbed on the Au rod, independently of the presence of oxygen vacancies (Fig. S2, Supporting Information). CO adsorption energies are in the range of -0.80 to -1.09 eV. The CO adsorption is about 0.15 eV more exothermic in the presence of the vacancy, the C-O bond length and the C-O stretching frequency on the other hand are not influenced by the presence of a single oxygen vacancy (Table S2, Supporting Information).

The next step consists of the abstraction of a lattice oxygen by reaction with the adsorbed CO molecule, where CO has to be located close to the Au/TiO_2 interface. We did not investigate the CO diffusion process on the Au particle, because CO diffusion on the gold rod should exhibit only minor barriers of around 0.5 eV.[29] To investigate the TiO_2 lattice oxygen abstraction, we chose to consider in more detail the formation of vacancy V_O 1–a located at the perimeter of the Au_{10}/TiO_2 interface (Fig. S1(a), Supporting Information). The reaction mechanism for the oxygen abstraction process is illustrated in Fig. 2. First, CO adsorbs on the Au rod, which releases 0.8 eV. Then, the CO molecule approaches the interface, giving an intermediate (Fig. 2, (c)). The next step is the removal of a TiO_2 lattice oxygen (Fig. 2 (c-e)). This process is approximately thermo-neutral, but exhibits an activation barrier of +0.97 eV. In Fig. 2 (c-e) we see that the lattice oxygen is removed in a concerted movement of the CO molecule, the surface oxygen atom and the gold rod. The last step consists of the desorption of the CO_2 molecule, which is endothermic by 0.80 eV. These calculations indicate that the first part of the catalytic cycle requires activation by about 1 eV.

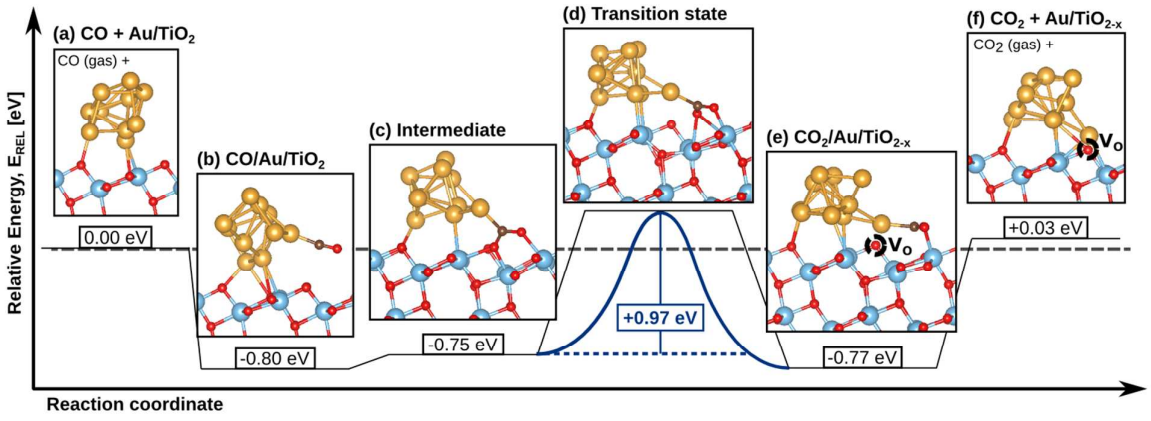

Fig. 2: CO oxidation via abstraction of a titania surface lattice oxygen. Relative energies are given with respect to the reactants shown in (a). (b-c) The CO molecule adsorbs and approaches the gold-titania interface. (c-e) CO abstracts a lattice oxygen and a gold atom 'refills' the oxygen vacancy. This process has an activation barrier of 0.97 eV. (f) The desorption of the CO_2 molecule is endothermic by 0.8 eV.

The presence of a barrier for the oxygen abstraction is in good agreement with the experiment, where CO_2 formation is increasingly hindered with decreasing temperature and almost completely inhibited at around -20°C.[35] Clearly, the barrier for the removal of titania lattice oxygen will depend on the particular chemical environment of the oxygen atom. There are three chemically different types of oxygen atoms on the titania anatase (101) surface: one two-fold coordinated species (2c-O), and two three-fold coordinated oxygen atoms (3c-O). Furthermore, the relative position of the oxygen atoms with respect to the Au rod, and the fluxionality of the rod will have an important effect both on the value of the barrier and on the stability of the formed oxygen vacancy. Nevertheless, the order of magnitude of the computed result agrees very well with the experimental observation that surface lattice oxygen removal is activated at about room temperature.

3.2 Re-oxidation of the catalyst

After the reduction of the catalyst by CO, the catalyst is re-oxidized by O_2 pulses (Fig. 1). The reduction by CO and re-oxidation by O_2 are reversible with stoichiometric amounts of CO and O_2 being consumed in consecutive pulse sequences. This is true except for the first sequence of multiple CO/Ar pulses directly after calcination (O400), which includes also the irreversible removal of oxygen from the surface of the Au nanoparticles (non-catalytic CO_2 formation), which was present after the initial calcination.[85] To investigate the temperature dependence of the re-oxidation step, we first reduced the catalyst by CO/Ar pulses at 240°C, followed by O_2/Ar pulses at different temperatures. The accumulated amounts of oxygen consumption during the O_2/Ar pulse sequences at different temperatures are shown in Fig. 3. At 240°C, the total amount of oxygen consumed during the whole sequence is around $1.3 \cdot 10^{18}$ O atoms g_{cat}^{-1}. Interestingly, the oxygen uptake at all other temperatures down to -80°C is only slightly lower than the uptake at 240°C.

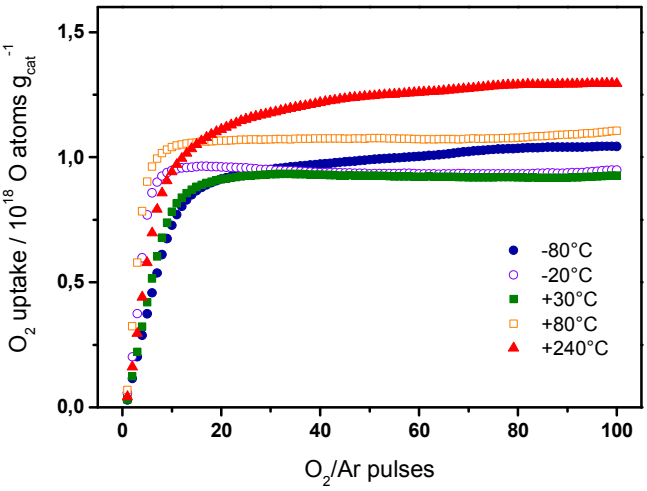

Fig. 3: Absolute, accumulated amounts of O_2 consumption during re-oxidation of Au/TiO_2 by O_2/Ar at various temperatures between -80°C and 240°C, where each of the re-oxidation experiments was performed directly after the catalyst reduction by CO/Ar at 240°C.

The total oxygen consumptions during O_2/Ar pulse sequences at different temperatures (-80° to 240°C), after the catalyst reduction at 240°C, are illustrated as filled columns in Fig. 4. They show almost identical oxygen consumption with $(1.0\pm0.1)\cdot10^{18}$ O atoms g_{cat}^{-1}, with a slightly higher value only at 240°C. The slightly lower values at temperatures below 240°C are tentatively assigned to a re-oxidation during the cooling process, e.g. by residual traces of water in the sample environment. The fact that the total oxygen consumption as well as the initial re-oxidation rate (after catalyst reduction at 240°C) are roughly temperature independent clearly demonstrates that the re-oxidation of the reduced Au/TiO_2 catalyst readily takes place also at low temperatures. This is in stark contrast to the activated removal of TiO_2 surface lattice oxygen, which was found to decay with decreasing temperature, until it is eventually completely inhibited at temperatures of -20°C and below.[35] If the catalyst is reduced at a temperature lower than 240°C, less oxygen is abstracted from the catalyst. This is illustrated by plotting the total reversible oxygen removal and oxygen consumption upon reduction by CO and re-oxidation by O_2 pulses at the same temperatures, which is indicated by empty columns for the respective temperatures in Fig. 4.

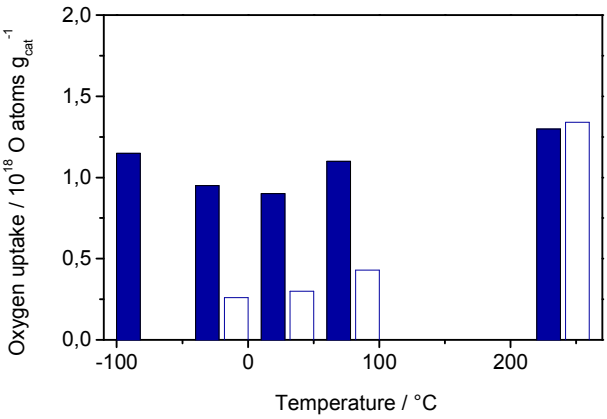

Fig. 4: *Filled columns:* Absolute amounts of O_2 consumption during re-oxidation of Au/TiO_2 by O_2/Ar at various temperatures between -80°C and 240°C, always directly after reduction by CO/Ar at 240°C. *Empty columns:* For comparison, we also show the reversible oxygen removal / oxygen uptake during reduction and re-oxidation by CO and O_2 pulses, respectively, at the same temperature.

On a quantitative scale, the O_2 uptake during O_2 pulsing, i.e., during re-oxidation, is shown in Fig. 5 for three different re-oxidation temperatures (240°C, 30°C, -80°C). It shows the fractional consumption of the O_2 pulses during re-oxidation. Obviously, independent of the temperature there is an essentially complete consumption of all O_2 molecules during the first ca. 5 O_2/Ar pulses. Afterwards, this decreases due to the lower amount of accessible oxygen vacancies still present. After around 25-30 pulses there is almost no more O_2 consumption at each temperature and, hence, the catalyst is close to being fully oxidized again. Using the O_2 pulse sizes (see Fig. S3, Supporting Information), the relative consumption during the O_2 pulses can be converted into absolute numbers of O_2 molecules, which are plotted in Fig. 5.

These results in total clearly demonstrate that the re-oxidation process of the reduced Au/TiO_2 catalysts is almost independent of the re-oxidation temperature. Accordingly, the effective

activation barrier for the replenishment of TiO_2 surface lattice oxygen vacancies at / close to the Au-TiO_2 perimeter sites under present reaction conditions (-80 to +240°C) must be negligible or even absent, in contrast to the activated surface lattice oxygen removal by CO. Based on these experimental results, the Au assisted Mars-van Krevelen mechanism is clearly limited by the activated removal of the active oxygen species from the perimeter sites, while re-oxidation is facile.

Similar to the vacancy formation process, the process of re-oxidation was simulated also computationally. Obviously, for the stoichiometric CO oxidation reaction, 2 CO + O_2 → 2 CO_2, two CO molecules are oxidized per O_2 molecule (Fig. 1). In the experiment, the re-oxidation is realized with molecular oxygen. Accordingly, we need two (neighboring) oxygen vacancies for the consumption of a single O_2 molecule. Alternatively, only a single vacancy is re-oxidized, and the other oxygen atom converts into an adsorbed oxygen (O_{ad}) species. This second oxygen species may either react with a second CO_{ad}, or with another oxygen vacancy. We first considered the latter case by investigating the

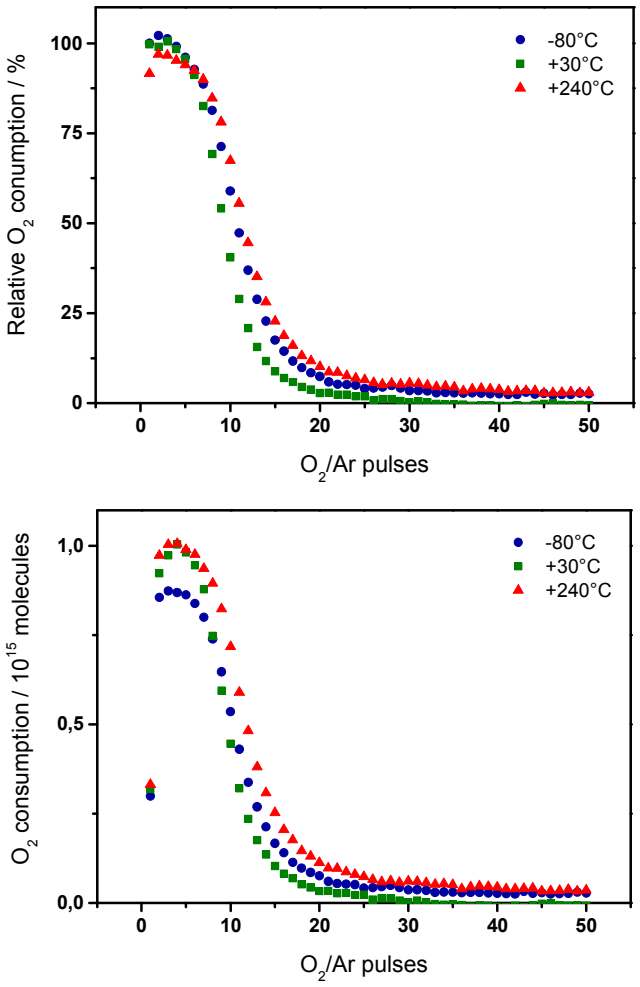

Fig. 5: Oxygen consumption relative to the O_2 pulse size (upper panel) and absolute amount of oxygen consumption (lower panel) during the re-oxidation of previously reduced Au/TiO_2 by O_2/Ar pulses at -80°C, 30°C, and 240°C.

replenishment of different isolated oxygen vacancies, both for the Au_{10}/TiO_2 **(Fig 6** (a.1-2)), and for the Au_{24}/TiO_2, (Fig 6 (b.1-2)) model systems. An example for the replenishment of two adjacent oxygen vacancies is then considered for Au_{10}/TiO_2 in Fig. 6 (a.3).

Let us consider in more detail the re-oxidation of the single oxygen vacancy V_O 1–a, Fig. 6 (a.1), which was formed in the process shown in Fig. 2. The formation energy of V_O 1–a at the Au_{10}/TiO_2 perimeter was reduced by 1.32 eV with respect to the Au-free surface. The energetics of the re-oxidation process is illustrated in Fig. 7. We start with the adsorption of molecular oxygen close to the vacancy, which is quite exothermic with an O_2 adsorption energy of around 2 eV (Fig. 7 (b)). After adsorption, the oxygen molecule dissociates. This process is exothermic by around 1.5 eV, and exhibits an activation barrier of 0.16 eV only (Fig. 7 (c)). Then, one of the oxygen atoms refills the vacancy, an exothermic process, which, however, exhibits a significant activation barrier of around 0.9 eV (Fig. 7 (d)). Overall, there is a large energy release associated to the adsorption and dissociation of the oxygen molecule

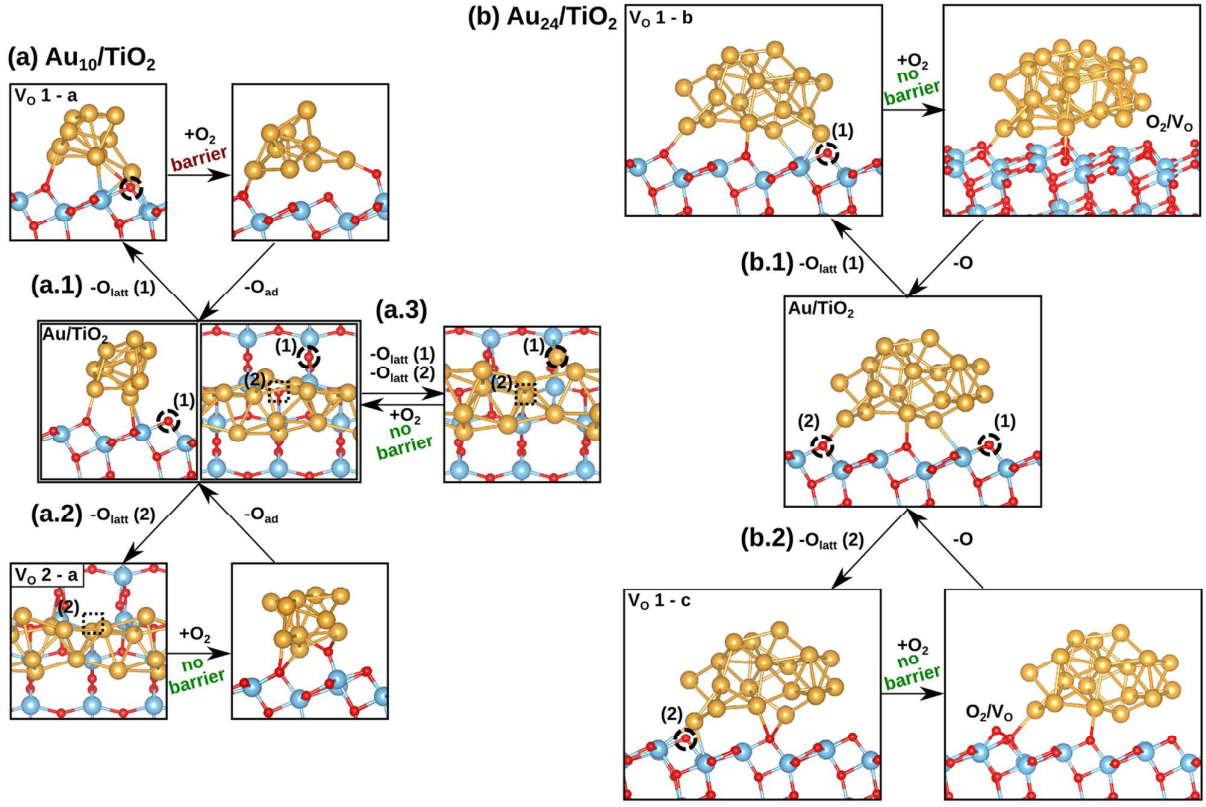

Fig. 6: (a) Reoxidation of Au_{10}/TiO_{2-x}. (a.1) Reoxidation of V_O 1–a under formation of $Au_{10}/O_{ad}/TiO_2$. (a.2) Reoxidation of vacancy V_O 2–a in combination with the formation of an O adatom ($Au_{10}/O_{ad}/TiO_2$). (a.3) Re-oxidation of two adjacent oxygen vacancies (V_O 1–a and V_O 2–a). (b) First step of the re-oxidation of Au_{24}/TiO_{2-x}. (b.1) Oxygen adsorption in V_O 1– b under formation of O_2/V_O. (b.2) Oxygen adsorption in V_O 1–c under formation of O_2/V_O. The oxygen vacancies are denoted according to their type and formation energy, see Table S1, Supporting Information.

(around 3.4 eV in total) but also a substantial barrier (activated process, in contrast to the experiment).

After the reaction shown in Fig. 7, the catalyst remains with an additional oxygen adatom (O_{ad}) at the Au/TiO_2 interface. As described above, this O_{ad} can (1) diffuse to another vacancy, or (2) a vacancy can diffuse to the O_{ad}, or (3) the oxygen adatom can be abstracted by reaction with a second CO_{ad} molecule. In the following, we will shortly go through these three possibilities. Let us first consider the option of O_{ad} migration. The O_{ad} is strongly bound with an adsorption energy of -1.80 eV with respect to ½ O_2. To obtain a stoichiometric oxidation, these oxygen adatoms could migrate to an oxygen vacancy and then refill it. We did not address this pathway computationally, as we assume that either the O_{ad} surface diffusion barrier is sufficiently low that the O_{ad} species can reach another vacancy and replenish it, or that O_{ad} rapidly reacts with CO_{ad} to form CO_2.

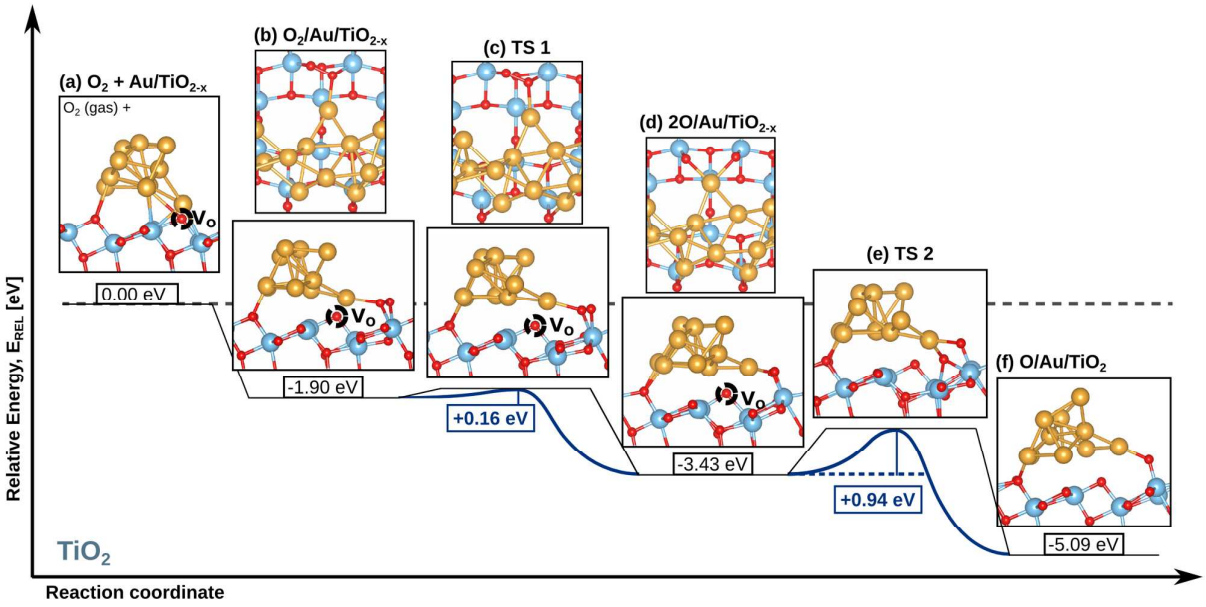

Fig. 7: Refilling of an oxygen vacancy on Au/TiO_2. (a-b) O_2 is molecularly adsorbed at the gold-titania interface, close to the oxygen vacancy. (c-d) The O_2 molecule dissociates with an activation barrier of 0.16 eV. (d-f) One of the oxygen atoms refills the vacancy. (e) This process includes a barrier of 0.94 eV. (f) A single oxygen adatom (O_{ad}) remains at the Au/TiO_2 interface.

The option of vacancy diffusion was investigated by A. Selloni and U. Diebold et. al. for Au-free titania anatase. They found that the vacancy migration in bulk titania anatase exhibits activation barriers of only around 0.2 eV.[86] To diffuse to the (101) surface, a barrier as large as 1.6 eV was found.[86] On the other hand, Wahlström et al. have shown that surface vacancies can easily migrate to a position underneath the Au particle on TiO_2-rutile (110).[87]

As a third option, we investigated the possibility to abstract the O_{ad} by reaction with CO. This process involves several steps, including the formation of a quite stable O-Au-CO intermediate (Fig. 8). Wang et al. also reported the formation of the O-Au-CO species during CO oxidation on a Au_{20} cluster supported on rutile TiO_2 (110).[49] Based on an exploratory

NEB calculation with a force-threshold of |0.1| eV/Å, we estimate an activation barrier of roughly 1 eV for the O_{ad} abstraction by CO. The complete catalytic cycle involving the O_{ad} abstraction by CO is summarized in (Fig. 8). In all three cases described above the re-oxidation involves an activation barrier at some point, which is in contradiction with the experimental findings.

Contrary to the case discussed above, the replenishment of the vacancy V_O 2–a on Au_{10}/TiO_2 (Fig. 6 (a.2)), proceeds via the spontaneous dissociation of the O_2 molecule, once this is brought into the vicinity of the vacancy. This is a result of the fact that the vacancy is not largely refilled by an Au atom from the rod, as it was the case for the vacancy V_O 1–a. The re-oxidation process involving the formation of an O_{ad} (Fig. 6 (a.2)), is exothermic by 4.59 eV with respect to the gas phase O_2 molecule. As in the previous case, the re-oxidation process leaves behind an oxygen adatom, which has to be consumed in some way. Hence, also in this case, re-oxidation involves an activated step with a barrier of around 1 eV, for the reaction of the O_{ad} species with CO_{ad}.

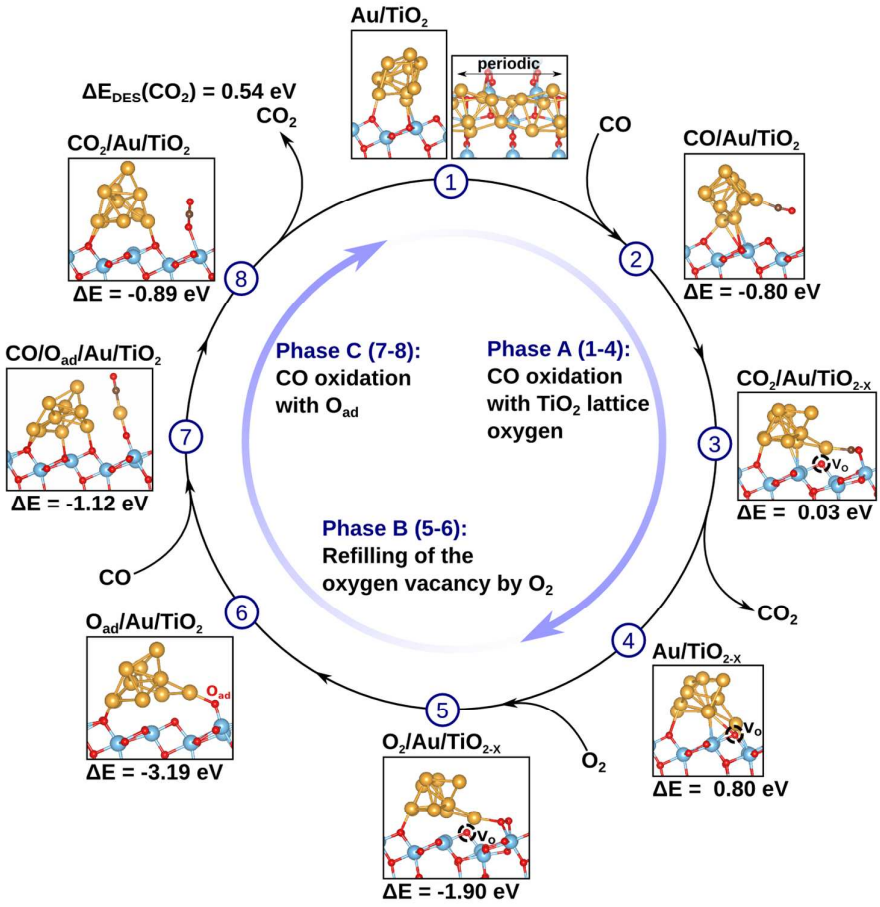

Fig. 8: Possible catalytic cycle for CO oxidation on $Au10/TiO_2$ involving the formation of a single oxygen vacancy and one oxygen adatom. In phase A, a titania lattice oxygen is abstracted by CO, forming CO_2 and an oxygen vacancy. In phase B, the oxygen vacancy is re-oxidized by O_2, leaving an oxygen adatom O_{ad} at the Au/TiO_2 interface. In phase C, the oxygen adatom O_{ad} is abstracted by CO, under formation of the second CO_2 molecule.

Let us now consider the other case for the re-oxidation at low vacancy concentration at the perimeter of the Au particle. Here, we investigated the replenishment of two different vacancy positions at the Au_{24}/TiO_2 perimeter (Fig. 6 (b.1-2)). As mentioned before, the fluxionality of the Au particle plays an important role in the vacancy stabilization and thus in the Au-assisted Mars-van Krevelen mechanism. In Fig. 6 (b.1-2), we see that the oxygen vacancies are only partly refilled by a Au atom from the rod, in the sense that only one of the under-coordinated Ti atoms from the vacancy is close enough to bind to the Au atom from the rod. It seems that the larger Au_{24} rod is less flexible than the Au_{10} rod. This makes the vacancy more accessible for the O_2 molecule, which readily adsorbs inside the vacancy without dissociating, similar as on the Au-free surface.[86] As this situation is similar to the Au-free surface, we assume a larger barrier for O_2 dissociation.

As a last case, we consider the high vacancy concentration regime, where adjacent vacancies are present, as shown in Fig. 6 (a.3). The formation energy of V_O 2–a at the Au_{10}/TiO_2 interface is 4.20 eV when vacancy V_O 1–a is already present. This is 1.7 eV less than on the Au-free surface. This further emphasizes the essential role of the Au particle to reduce the cost of O vacancy formation. In this case, the two vacancies are re-oxidized spontaneously upon adsorption of the O_2 molecule. The resulting catalytic cycle for CO oxidation involving the formation of two adjacent vacancies is summarized in Fig. 9. As the process is barrierless, we desist from showing an additional energy diagram as in Fig. 7 and summarize the process in Fig. 9 (phase 5 $\rightarrow$ 1). The computational findings for the high vacancy coverage regime are in perfect agreement with experimental findings.

The data presented and discussed so far clearly indicate that the results of the TAP reactor pulse sequences can be reproduced theoretically. In both cases the removal of surface lattice oxygen at the perimeter sites is activated, and the size of the computed kinetic barrier, which for a number of different configurations is around 1.0 eV, fits well to the experimental results. In fact, a lower barrier in the calculations would be in contrast to the experimental observations, since it would not be able to explain the observed decay of the efficiency for lattice oxygen removal, which is essentially fully hindered at -20°C.

On the other hand, for the re-oxidation of the surface oxygen vacancies, which based on experimental observations proceeds essentially barrierless, calculations also yielded a substantial barrier when performed with a single vacancy, i.e., in the limits of low surface oxygen vacancy concentrations. This situation would be typical for reaction gas mixtures with an excess of O_2 in the gas phase, i.e., at a O_2 : CO ratio of 0.5 and higher [88]. A barrier-free process, on the other hand, was observed in the presence of 2 adjacent vacancies. This situation would become increasingly probable for lower O_2 : CO ratios, well below stoichiometric composition. Here we have to keep in mind that the number of configurations tested for this process was rather limited, and it may well be that there are other single-vacancy configurations which also show a very low barrier for re-oxidation of the surface oxygen vacancies. This would also be in better agreement with the experimental observation that increasing the oxygen excess mostly leads to an increased CO oxidation rate, resulting in a positive reaction order for O_2.[89]

As discussed above, the barrier for re-oxidation is mainly associated with the filling of the O surface vacancy rather than with the dissociation. For the continuous reaction one could therefore envision a reaction process where the formation of vacancies is responsible for facile dissociation of molecularly adsorbed $O_{2,ad}$ in the vicinity of a vacancy, but where in a next step both of the resulting atomic oxygen species react with CO instead of filling this vacancy, which as discussed above is a significantly activated step. The resulting barrier for the reaction of CO_{ad} and O_{ad} in the presence of an oxygen vacancy may be lower than in the absence of a vacancy, which was estimated above to be about 1.0 eV. This process would be rather similar to the reaction mechanism proposed by Vilhelmsen and Hammer,[41;44] who also proposed an atomic oxygen species as reactive species. In their case, however, oxygen dissociation was activated by a highly oxidized interface, whereas in our case this activation would be due to surface lattice oxygen vacancies at the perimeter sites.

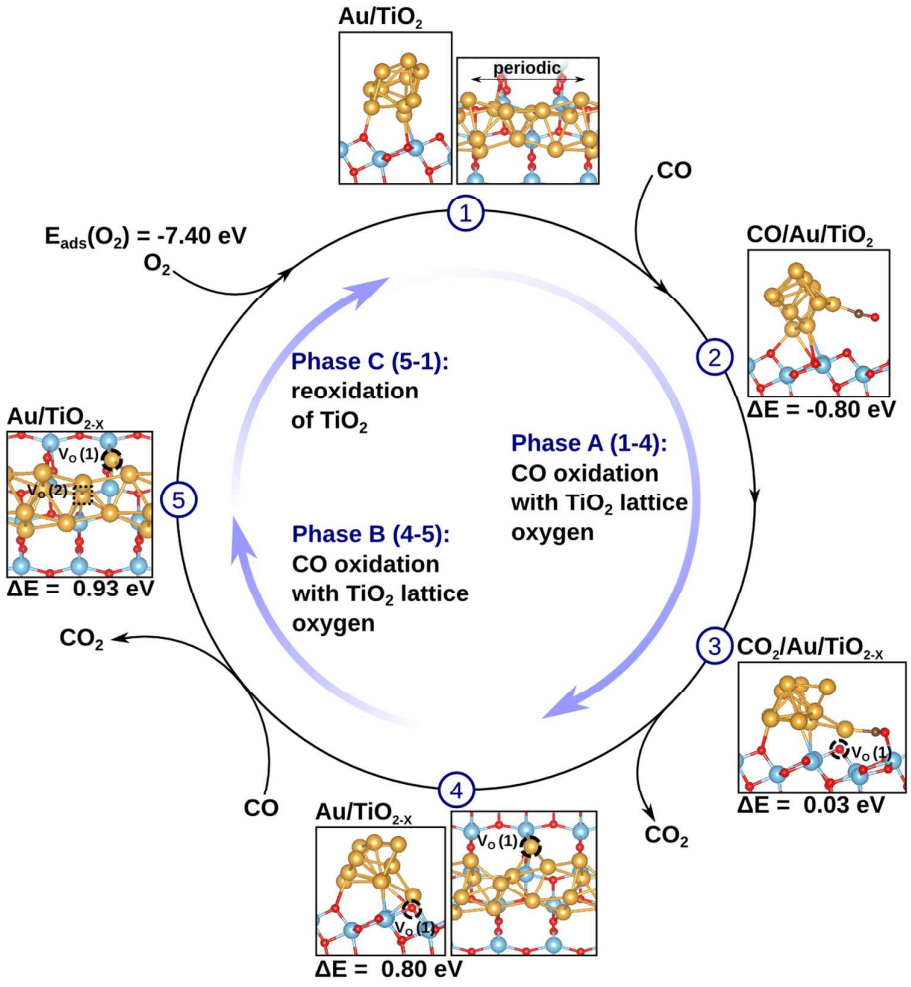

Fig. 9: Possible catalytic cycle for CO oxidation involving the formation of two adjacent oxygen vacancies. In phase A, the first titania lattice oxygen is abstracted by CO, forming CO_2 and an oxygen vacancy. In phase B, the second lattice oxygen is abstracted by CO, forming a second CO_2. In phase C, the two vacancies are refilled by O_2.

While we cannot rule out the process proposed by Vilhelmsen and Hammer for continuous reaction, it can hardly explain the results of the TAP reactor pulse sequences. In the latter case, reduction by CO pulses would not only remove the oxygen adatoms formed upon O_2 dissociation close to the oxidized interface, but also the interface oxygen, at least those interface oxygen species which are close to the perimeter sites. As a consequence, the highly oxidized interface, which is essential for facile O_2 dissociation, is no longer present, and O_2 dissociation should become increasingly activated, in contrast to experimental observations (see Fig. 5). In conclusion, while we cannot rule out this mechanism for the continuous CO oxidation reaction on Au/TiO_2 at present, in particular under highly oxidizing conditions, it is not compatible with the results of the multi-pulse experiments. Similar arguments apply also to the reaction mechanism proposed Duan and Henkelman, which also requires the presence of an oxidized interface.[47] The Au assisted Mars – van Krevelen considered here, on the other hand, is compatible with both reaction conditions, continuous reactions and sequential reaction in the multi-pulse experiments. In that case it is likely that this also contributes significantly to the continuous CO oxidation reaction. This will be explored further in ongoing work.

Finally we would like to briefly comment on discrepancies between the reaction barrier of about 1 eV derived from the present work, both experimentally and theoretically, and the barriers derived from temperature dependent rate measurements. These latter experiments resulted in a wide range of activation barriers, which also varied with temperature.[89-91] First of all it should be noted that depending on the reaction conditions such measurements lead to values which may be anywhere between the actual activation barrier in the elementary CO oxidation process, and the apparent activation energy, which represents the difference between reaction barrier and CO desorption barrier.[92] For the present case of weak O_2 adsorption the O_2 desorption barrier may participate as well. Hence, the values derived from such measurements may i) be quite different from the barrier derived for the activated elementary step, and ii) it may vary significantly depending on the actual experimental situation. This should be considered when comparing our findings with experimental data.

4. Conclusions

Aiming at a microscopic understanding of the continuous CO oxidation on a Au/TiO_2 catalyst under typical reaction conditions, at ambient temperature and above, we have explored mechanistic aspects of this reaction in a combined experimental and computational study. This leads us to the following main results and conclusions:

1. The activated removal of titania surface lattice oxygen by reaction with CO, which was proposed by previous TAP reactor measurements, is confirmed by atomistic reaction models based on DFT calculations. These calculations reveal a significant reduction of the oxygen vacancy formation energies (by up to 2.2 eV) at the Au/TiO_2 anatase (101) interface perimeter compared to the Au-free TiO_2 surface. The Au particles closely interact with the vacancies, whereby a charge transfer from the vacancy to the Au particle occurs. The ability of the Au particles to accommodate the excess electrons associated to the vacancies formed at the Au/TiO_2 perimeter and the coordination of the vacancy Ti

atoms by Au leads to a stabilization of the vacancies, lowering both the vacancy formation energies and the kinetic barriers for vacancy formation. Lowering of the vacancy formation energy does not require the presence of an oxidized interface

2. According to the calculations, the Au-assisted CO oxidation can proceed as follows: CO is adsorbed on the Au particle with an adsorption energy of around -0.8 eV; CO then abstracts a TiO_2 lattice oxygen at the Au/TiO_2 anatase (101) perimeter with an activation barrier of around 1.0 eV. In the last step, CO_2 desorbs, leaving behind an oxygen vacancy, i.e. the reduced catalyst Au/TiO_{2-x}. The CO_2 desorption process is endothermic by around 0.8 eV, which is identical with the kinetic barrier for this process. Hence, the reactive removal of surface lattice oxygen is the rate determining step, in particular at ambient temperatures or slightly above.

3. The next step in the Au-assisted Mars - van Krevelen mechanism involves the re-oxidation of the previously reduced catalyst. Multi-pulse TAP measurements, performed on a catalyst pre-reduced by CO pulses at 240°C, reveal that neither the total amount of oxygen uptake, nor the (initial) uptake kinetics change significantly in the temperature range between -80°C and 240°C. These findings clearly indicate the absence of an activation barrier for the re-oxidation process. Computationally, we explored various possible re-oxidation processes and found that the re-oxidation of the catalyst can proceed barrierless in the case of two adjacent vacancies at the perimeter, i.e., at higher oxygen vacancy concentration at the Au/TiO_2 perimeter. In this case the O_2 molecule can split spontaneously and refill both vacancies. The replenishment of a single oxygen vacancy by O_2 (low vacancy concentration) leads to the formation of oxygen adatoms (O_{ad}) at the Au/TiO_2 perimeter. In this case calculations predict a significant barrier for the re-oxidation process, either for the surface migration of a vacancy, or for the abstraction of O_{ad} by CO. Lower barriers for configurations not tested here cannot be excluded.

Overall, these results further support previous proposals of a Au assisted Mars – van Krevelen mechanism for the CO oxidation on Au/TiO_2 catalysts under typical reaction conditions, at ambient temperatures and above. Furthermore, they underline the importance of including activation barriers and considering the full catalytic cycle in mechanistic proposals and computational studies. Finally, they emphasize the specific role of Au for facilitating the formation of oxygen lattice vacancies, since Au can easily accept and stabilize the electron generated during that process.

Notes

The authors declare no competing financial interest.

Acknowledgments

The work of PS and GP has been supported by the European Community's Seventh Program FP7/2007–2013 under Grant Agreement nº 607417 – European Marie Curie Network CATSENSE, and by the Italian MIUR through the PRIN Project 2015K7FZLH SMARTNESS "Solar driven chemistry: new materials for photo– and electro–catalysis".

References

(1) Haruta, M.; Daté, M. *Appl. Catal. A* **2001**, 222, 427-437.

(2) Hashmi, A. S. K.; Hutchings, G. J. *Angew. Chem. Int. Ed.* **2006**, 45, 7896-7936.

(3) Corma, A.; Garcia, H. *Chem. Soc. Rev.* **2008**, 37, 2096-2126.

(4) Hutchings, G. J.; Brust, M.; Schmidbaur, H. *Chem. Soc. Rev.* **2008**, 37, 1759-1765.

(5) Haruta, M.; Kobayashi, T.; Sano, H.; Yamada, N. *Chem. Lett.* **1987**, 16, 405-408.

(6) Hutchings, G. J. *Gold Bull.* **1996**, 29, 123-130.

(7) Bond, G. C.; Thompson, D. T. *Catal. Rev. Sci. Eng.* **1999**, 41, 319-388.

(8) Kung, M. C.; Costello, C.; Kung, H. H. *Catalysis* **2004**, 17, 152.

(9) Janssens, T. V. W.; Clausen, B. S.; Hvolbaek, B.; Falsig, H.; Christensen, C. H.; Bligaard, T.; Nørskov, J. K. *Top. Catal.* **2007**, 44, 15-26.

(10) Andreeva, D. *Gold Bull.* **2002**, 35, 82-88.

(11) Fu, Q.; Saltsburg, H.; Flytzani-Stephanopoulos, M. *Science* **2003**, 301, 935-938.

(12) Deng, W.; Flytzani-Stephanopoulos, M. *Angew. Chem.* **2006**, 118, 2343-2347.

(13) Chen, Y.; Wang, H.; Burch, R.; Hardacre, C.; Hu, P. *Faraday Discuss.* **2011**, 152, 121-133.

(14) Wang, L.-C.; Widmann, D.; Behm, R. J. *Catal. Sci. Technol.* **2015**, 5, 925-941.

(15) Flytzani-Stephanopoulos, M. *Acc. Chem. Res.* **2014**, 47, 783-792.

(16) Haruta, M. *Catal. Today* **1997**, 36, 153-166.

(17) Grisel, R. J. H.; Nieuwenhuys, B. E. *Catal. Today* **2001**, 64, 69-81.

(18) Min, B. K.; Friend, C. M. *Chem. Rev.* **2007**, 107, 2709-2724.

(19) Sakurai, H.; Haruta, M. *Appl. Catal. A* **1995**, 127, 93-105.

(20) Strunk, J.; Kähler, K.; Xia, X.; Comotti, M.; Schüth, F.; Reinecke, T.; Muhler, M. *Appl. Catal. A* **2009**, 359, 121-128.

(21) Yang, Y.; Mei, D.; Peden, C. H. F.; Campbell, C. T.; Mims, C. A. *ACS Catal.* **2015**, 5, 7328-7337.

(22) Hartadi, Y.; Widmann, D.; Behm, R. J. *J. Catal.* **2016**, 333, 238-250.

(23) Derrouiche, S.; La Fontaine, C.; Thrimurtulu, G.; Casale, S.; Delannoy, L.; Lauron-Pernot, H.; Louis, C. *Catal. Sci. Technol.* **2016**, 6, 6794-6805.

(24) Freund, H. J.; Meijer, G.; Scheffler, M.; Schlögl, R.; Wolf, M. *Angew. Chem. Int. Ed.* **2011**, 50, 10064-10094.

(25) Kung, H. H.; Kung, M. C.; Costello, C. K. *J. Catal.* **2003**, 216, 425-432.

(26) Akita, T.; Okumura, M.; Tanaka, K.; Ohkuma.K.; Kohyama, M.; Koyanagi, T.; Daté, M.; Tsubota, S.; Haruta, M. *Surf. Interf. Anal.* **2005**, 37, 265-269.

(27) Daniells, S. T.; Overweg, A. R.; Makkee, M.; Moulijn, J. A. *J. Catal.* **2005**, 230, 52-65.

(28) Fierro-Gonzalez, C.; Guzman, J.; Gates, B. C. *Top. Catal.* **2007**, 44, 103-114.

(29) Green, I. X.; Tang, W.; Neurock, M.; Yates, J. T. *Science* **2011**, 333, 736-739.

(30) Widmann, D.; Behm, R. J. *Angew. Chem. Int. Ed.* **2011**, 50, 10241-10245.

(31) Maeda, Y.; Iizuka, Y.; Kohyama, M. *J. Am. Chem. Soc.* **2013**, 135, 906-909.

(32) Saavedra, J.; Doan, H. A.; Pursell, C. J.; Grabow, L. C.; Chandler, B. D. *Science* **2014**, 345, 1599-1602.

(33) Widmann, D.; Behm, R. J. *Acc. Chem. Res.* **2014**, 47, 740-749.

(34) Green, I. X.; Tang, W.; Neurock, M.; Yates, J. T. *Acc. Chem. Res.* **2014**, 47, 805-815.

(35) Widmann, D.; Krautsieder, A.; Walther, P.; Brückner, A.; Behm, R. J. *ACS Catal.* **2016**, 6, 5005-5011.

(36) Schilling, C.; Hess, C. *Top. Catal.* **2017**, 60, 131-140.

(37) Molina, L. M.; Hammer, B. *Phys. Rev. Lett.* **2003**, 90, 206102-1-206102-4.

(38) Remediakis, I. N.; Lopez, N.; Nørskov, J. K. *Angew. Chem.* **2005**, 117, 1858-1860.

(39) Laursen, S.; Linic, S. *Phys. Chem. Chem. Phys.* **2009**, 11, 11006-11012.

(40) Kim, H. Y.; Henkelman, G. *J. Phys. Chem. Lett.* **2013**, 4, 216-221.

(41) Vilhelmsen, L. B.; Hammer, B. *J. Chem. Phys.* **2013**, 139, 204701.

(42) Wang, Y. G.; Yoon, Y.; Glezakou, V. A.; Li, J.; Rousseau, R. *J. Am. Chem. Soc.* **2013**, 135, 10673-10683.

(43) Li, L.; Zeng, X. C. *J. Am. Chem. Soc.* **2014**, 136, 15857-15860.

(44) Vilhelmsen, L. B.; Hammer, B. *ACS Catal.* **2014**, 4, 1626-1631.

(45) Saqlain, M. A.; Hussain, A.; Siddiq, M.; Ferreira, A. R.; Leitao, A. A. *Phys. Chem. Chem. Phys* **2015**, 17, 25403-25410.

(46) Wang, Y.-G.; Mei, D.; Glezakou, V. A.; Li, J.; Rousseau, R. *Nat. Commun.* **2015**, 6, 1-7.

(47) Duan, Z.; Henkelman, G. *ACS Catal.* **2015**, 5, 1589-1595.

(48) Saqlain, M. A.; Hussain, A.; Siddiq, M.; Ferreira, A. R.; Leitao, A. A. *Appl. Catal. A* **2016**, 519, 27-33.

(49) Wang, Y. G.; Cantu, D. C.; Lee, M. S.; Li, J.; Glezakou, V. A.; Rousseau, R. *J. Am. Chem. Soc.* **2016**, 138, 10467-10476.

(50) Wang, Y.; Lehnert, F.; Widmann, D.; Gu, D.; Schüth, F.; Behm, R. J. *Angew. Chem. Int. Ed.* **2017**, 56, 9597-9602.

(51) Wang, Y.; Widmann, D.; Wittmann, M.; Lehnert, F.; Gu, D.; Schüth, F.; Behm, R. J. *Catal. Sci. Technol.* **2017**, 7, 4145-4161.

(52) Kotobuki, M.; Leppelt, R.; Hansgen, D.; Widmann, D.; Behm, R. J. *J. Catal.* **2009**, 264, 67-76.

(53) Widmann, D.; Liu, Y.; Schüth, F.; Behm, R. J. *J. Catal.* **2010**, 276, 292-305.

(54) Wang, Y.; Widmann, D.; Heenemann, M.; Diemant, T.; Biskupek, J.; Schlögl, R.; Behm, R. J. *J. Catal.* **2017**, 354, 46-60.

(55) Li, L.; Wang, A.; Qiao, B.; Lin, J.; Huang, Y.; Wang, X.; Zhang, T. *J. Catal.* **2013**, 299, 90-100.

(56) Lohrenscheit, M.; Hess, C. *ChemCatChem* **2016**, 8, 523-526.

(57) Ruiz Puigdollers, A.; Schlexer, P.; Tosoni, S.; Pacchioni, G. *ACS Catal.* **2017**, 7, 6493-6513.

(58) Daté, M.; Haruta, M. *J. Catal.* **2001**, 201, 221-224.

(59) Satterfield, C. N. *Heterogeneous catalysis in industrial practice*; 1991; pp 1-554.

(60) Leppelt, R.; Hansgen, D.; Widmann, D.; Häring, T.; Bräth, G.; Behm, R. J. *Rev. Sci. Instrum.* **2007**, 78, 104103-1-104103-9.

(61) Kresse, G.; Hafner, J. *Phys. Rev. B* **1993**, 47, 558-561.

(62) Kresse, G.; Hafner, J. *Phys. Rev. B* **1994**, 49, 14251-14269.

(63) Kresse, G.; Furthmüller, J. *Comp. Mat. Sci.* **1996**, 6, 15-50.

(64) Kresse, G.; Furthmüller, J. *Phys. Rev. B* **1996**, 54, 11169-11186.

(65) Perdew, J. P.; Burke, K.; Ernzerhof, M. *Phys. Rev. Lett.* **1996**, 77, 3865-3868.

(66) Perdew, J. P.; Burke, K.; Ernzerhof, M. *Phys. Rev. Lett.* **1997**, 78, 1396.

(67) Dudarev, S. L.; Botton, G. A.; Savrasov, S. Y.; Humphreys, C. J.; sutton, A. P. *Phys. Rev. B* **1998**, 57, 1505-1509.

(68) Hu, Z. P.; Metiu, H. *J. Phys. Chem. C* **2011**, 115, 17898-17909.

(69) Finazzi, E.; Di Valentin, C.; Pacchioni, G.; Selloni, A. *J. Chem. Phys.* **2008**, 129, 154113.

(70) Blöchl, P. E. *Phys. Rev. B* **1994**, 50, 17953-17979.

(71) Kresse, G.; Joubert, D. *Phys. Rev. B* **1999**, 59, 1758-1775.

(72) Liu, B. Report on Workshop: Numerical Algorithms in Chemistry: Algebraic Methods. 1-171. 9-8-1978.

(73) Davidson, E. R. Matrix Eigenvector Methods; In *Methods in Computational Molecular Physics*; Diercksen, G. H. F., Wilson, S., eds. 1983; pp 95-113.

(74) Monkhorst, H. J.; Pack, J. D. *Phys. Rev. B* **1976**, 13, 5188-5192.

(75) Djerdj, I.; Tonejc, A. M. *J. Alloys Compd.* **2006**, 413, 159-174.

(76) Stoneham, A. M. *Appl. Surf. Sci.* **1983**, 14, 249-259.

(77) Ruiz Puigdollers, A.; Schlexer, P.; Pacchioni, G. *J. Phys. Chem. C* **2015**, 119, 15381-15389.

(78) Grimme, S. *J. Comput. Chem.* **2006**, 27, 1787-1799.

(79) Tosoni, S.; Sauer, J. *Phys. Chem. Chem. Phys.* **2010**, 12, 14330-14340.

(80) Sanville, E.; Kenny, S. D.; Smith, R.; Henkelman, G. *J. Comput. Chem.* **2007**, 28, 899-908.

(81) Tang, W.; Jayaraman, S.; Jaramillo, T. F.; Stucky, G. D.; McFarland, E. W. *J. Phys. Chem. C* **2009**, 113, 5014-5024.

(82) Henkelman, G.; Jónsson, H. *J. Chem. Phys.* **2000**, 113, 9978-9986.

(83) Yoon, B.; Häkkinen, H.; Landman, U.; Wörz, A. S.; Antonietti, M.; Abbet, S.; Judai, K.; Heiz, U. *Science* **2005**, 307, 403-407.

(84) Lin, X.; Yang, B.; Benia, H.-M.; Myrach, P.; Yulikov, M.; Aumer, A.; Brown, M. A.; Sterrer, M.; Bondaschurk, O.; Kieseritzky, E.; Rocker, J.; Risse, T.; Gao, H.-J.; Nilius, N.; Freund, H.-J. *J. Am. Chem. Soc.* **2010**, 132, 7745-7749.

(85) Widmann, D.; Behm, R. J. *Chin. J. Catal.* **2016**, 37, 1684-1693.

(86) Setvin, M.; Aschauer, U.; Scheiber, P.; Li, Y. F.; Hou, W.; Schmid, M.; Selloni, A.; Diebold, U. *Science* **2013**, 341, 988-991.

(87) Wahlström, E.; Kruse Vestergaard, E.; Schaub, R.; Ronnau, A.; Vestergaard, M.; Laegsgaard, E.; Stensgaard, I.; Besenbacher, F. *Science* **2004**, 303, 511-513.

(88) Widmann, D.; Behm, R. J. *J. Catal.* **2018**, 357, 263-273.

(89) Schumacher, B.; Denkwitz, Y.; Plzak, V.; Kinne, M.; Behm, R. J. *J. Catal.* **2004**, 224, 449-462.

(90) Haruta, M.; Tsubota, S.; Kobayashi, T.; Kageyama, H.; Genet, M. J.; Delmon, B. *J. Catal.* **1993**, 144, 175-192.

(91) Bond, G. C.; Louis, C.; Thompson, D. T. Oxidation of Carbon Monoxide; In *Catalysis by Gold*; Bond, G. C., Louis, C., Thompson, D. T., eds. World Scientific: 2007; pp 161-203.

(92) Somorjai, G. A. *Introduction to Surface Science and Catalysis*; John Wiley and Sons: New York, 1994.

Table of Contents